Frontiers of tensor networks: from moiré materials to higher-order topology

Bartholomew Andrews

Research Overview, UCLA

April 6, 2021

University of Zurich UZH

FNSNF Swiss National Science Foundation

About Me

2015→2019: PhD, University of Cambridge
[G. Möller and G. Conduit]

2018→Now: Postdoc, University of Zurich
[A. Soluyanov and T. Neupert]

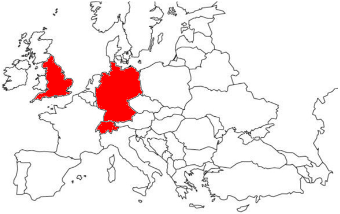

Research Interests:

- fractional Chern insulators
- stability of molecules/crystals
- moiré materials
- higher-order topology

Software Development:

- exact diagonalization [DiagHam]
- quantum Monte Carlo [CASINO]
- tensor networks [TeNPy]

About Me

2015→2019: PhD, University of Cambridge

[G. Möller and G. Conduit]

2018→Now: Postdoc, University of Zurich

[A. Soluyanov and T. Neupert]

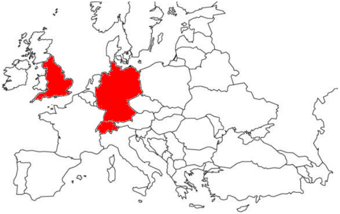

Research Interests:

- fractional Chern insulators
- stability of molecules/crystals
- moiré materials
- higher-order topology

Software Development:

- exact diagonalization [DiagHam]
- quantum Monte Carlo [CASINO]
- tensor networks [TeNPy]

I. Moiré Materials

Alexey Soluyanov

1983 – 2019

B. Andrews and A. Soluyanov, Phys. Rev. B **101**, 235312 (2020)

Motivation

Interest in **fractional quantum Hall (FQH)** states in moiré flatbands:

analytics

numerics

Fractional Chern Insulator States in Twisted Bilayer Graphene: An Analytical Approach

Patrick J. Ledwith, Grigory Tarnopolsky, Eslam Khalaf and Ashvin Vishwanath
Department of Physics, Harvard University, Cambridge, MA 02138, USA
(Dated: December 23, 2019)

Vishwanath's group, PRR **2**, 023237 (2020)

Particle-Hole Duality, Emergent Fermi Liquids and Fractional Chern Insulators in Moiré Flatbands

Ahmed Abouelkomsan[1], Zhao Liu[2*] and Emil J. Bergholtz[1†]
[1]*Department of Physics, Stockholm University, AlbaNova University Center, 106 91 Stockholm, Sweden*
[2]*Zhejiang Institute of Modern Physics, Zhejiang University, Hangzhou 310027, China*
(Dated: December 12, 2019)

Bergholtz's group, PRL **124**, 106803 (2020)

What happens in the presence of a perpendicular magnetic field $\Rightarrow$ **Hofstadter regime**?

- $\downarrow$ take an effective lattice model for low-energy flat bands
- $\downarrow$ enrich the physics by applying a magnetic field
- $\downarrow$ tune to topological flat mini-bands

What fractional states can emerge? Is Hofstadter physics reproduced?

Single-particle Hamiltonian

We consider an effective **two-orbital** Hubbard model[1] for **spinless fermions**, $\mathbf{c} = (c_x, c_y)$, hopping on a **honeycomb** moiré superlattice in a perpendicular magnetic field $\mathbf{B} = B\hat{\mathbf{e}}_z$.

$$H_0 = \sum_{\langle ij \rangle} \left[t_1 e^{i\theta_{ij}} \mathbf{c}_i^\dagger \cdot \mathbf{c}_j + \text{H.c.} \right] + \kappa \sum_{\langle ij \rangle_5} \left[t_2 e^{i\theta_{ij}} \mathbf{c}_i^\dagger \cdot \mathbf{c}_j + t_2' e^{i\theta_{ij}} (\mathbf{c}_i^\dagger \times \mathbf{c}_j)_z + \text{H.c.} \right]$$

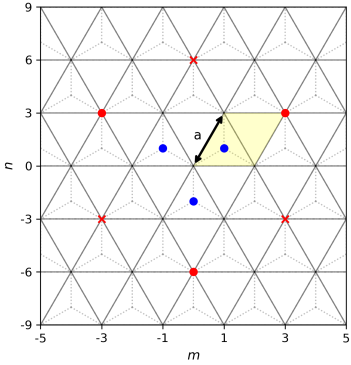

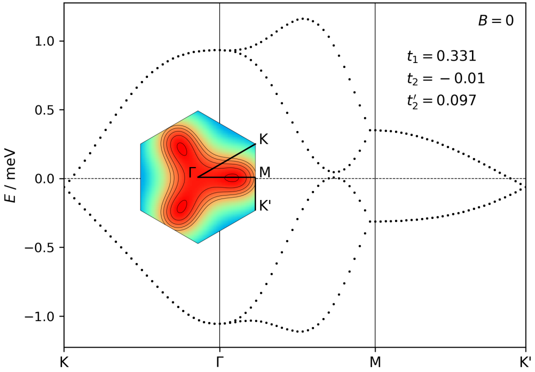

[1] Koshino et al., PRX **8**, 031087 (2018)

Single-particle Hamiltonian

We apply a magnetic field via a **Peierls substitution** such that $\theta_{ij} = (2\pi/\phi_0) \int_i^j \mathbf{A} \cdot \mathrm{d}\mathbf{l}$.

$$H_0 = \sum_{\langle ij \rangle} \left[t_1 e^{\mathrm{i}\theta_{ij}} \mathbf{c}_i^\dagger \cdot \mathbf{c}_j + \text{H.c.} \right] + \kappa \sum_{\langle ij \rangle_5} \left[t_2 e^{\mathrm{i}\theta_{ij}} \mathbf{c}_i^\dagger \cdot \mathbf{c}_j + t_2' e^{\mathrm{i}\theta_{ij}} (\mathbf{c}_i^\dagger \times \mathbf{c}_j)_z + \text{H.c.} \right]$$

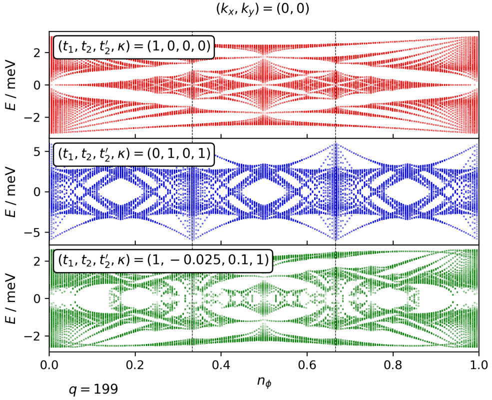

We define the **flux density** as

$$n_\phi = \frac{BA_{\text{UC}}}{\phi_0} \equiv \frac{p}{q},$$

where $A_{\text{UC}} = \sqrt{3}a^2/2$, $\phi_0 = h/e$, and p, q are coprime integers. The (in)commensurability of the areas scales for the **magnetic unit cell** and the **flux quantum** yields a fractal spectrum.

Many-body Hamiltonian

$$H = H_0 + \underbrace{\boxed{U \sum_i \rho_{x,i}\rho_{y,i}}}_{\text{inter-orbital}} + \underbrace{\boxed{V \sum_{\langle ij \rangle} \rho_i \rho_j}}_{\text{inter-site}}$$

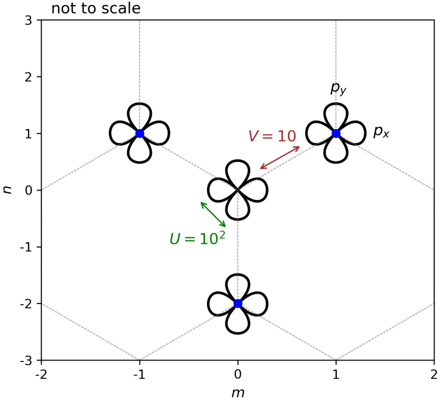

- Electronic Wannier orbitals span over multiple unit cells $\Rightarrow$ **interactions** are expected to play an **important** role.

$$E_C \sim \frac{e^2}{\epsilon L} \approx 10 - 40 \text{ meV}$$

- Typical screening by metallic gates in realistic devices $\Rightarrow$ **nearest-neighbor** interactions are expected to be **sufficient**[2].

[2] Yuan and Fu, PRB **98**, 045103 (2018)

Lattice geometries

To achieve a FQH state, we must select the correct lattice geometry and filling factor.

filling fraction of the system w.r.t. unit cells

$$\textbf{Filling factor}, \ \nu = \boxed{n}/\boxed{n_\phi} \equiv r/s$$

magnetic flux per unit cell, $n_\phi \equiv p/q$

Requirements	Constraints
+ large q to get flat bands	− larger q increases the area of the magnetic unit cell
+ large system size to minimize finite-size effects	− iDMRG computations scale $\sim L_x$ and $\sim \exp(L_y)$
+ large variety of lattice geometries to investigate scaling	− geometries limited by particle number and filling factor

Lattice geometries

Example: $\nu = 1/3$ state

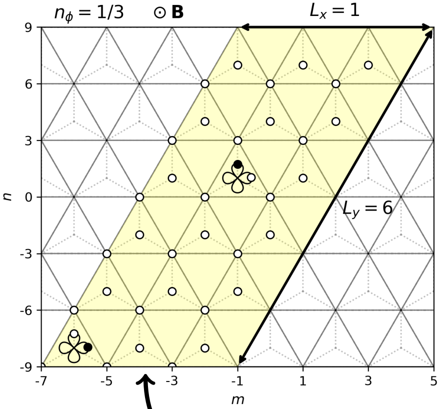

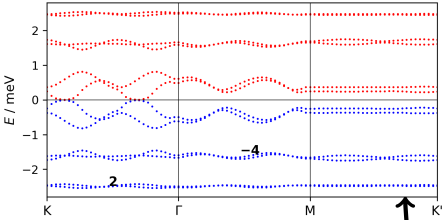

Orbital polarization ⇒ two quasi-degenerate $C = 1$ bands.

We expect a FQH state at filling

$$\nu = \frac{r}{|kC|r + 1} \stackrel{!}{=} \frac{1}{2 \times 1 + 1} = \frac{1}{3}$$

of the lowest quasi-degenerate band.

\# lattice sites = 36

\# orbital sites = 72

This corresponds to filling $^1/_{36}$ of the orbital sites in our system.

Evidence for the $\nu = 1/3$ state

...from flux insertion[3]

Charge pumping

Total charge pumped across the cut in the cylinder corresponds to the Hall conductivity $\sigma_H \propto C\nu$. ✓

Spectral flow

Entanglement energies flow into themselves after the insertion of s flux quanta, with the charge sector labeling shifted by $|C|r$. ✓

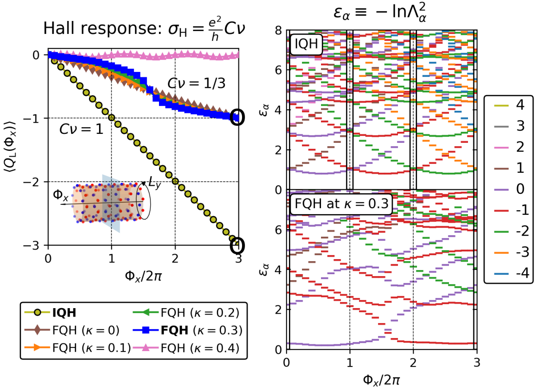

[3] Andrews and Soluyanov, PRB **101**, 235312 (2020)

Evidence for the $\nu = 1/3$ state

…from entanglement[3]

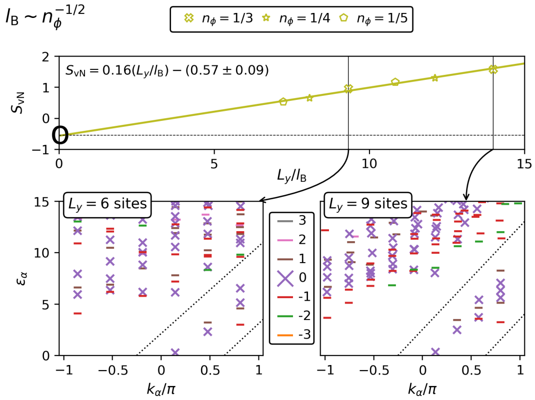

Entanglement scaling

From the 'area law':

$$S = cL_y - \gamma,$$

the topological entanglement entropy is given as

$$\gamma = \ln \sqrt{\sum_i d_i^2},$$

with $d_i = 1$ for Abelions. ✓

Edge counting

$U(1)$ conformal field theory predicts the ground-state counting $\{1, 1, 2, 3, \dots\}$ for each Q_L sector. ✓

[3] Andrews and Soluyanov, PRB **101**, 235312 (2020)

Orbital-polarized FQH breakdown

gap-to-width ratio

charge pumping

correlation length

entanglement spectrum

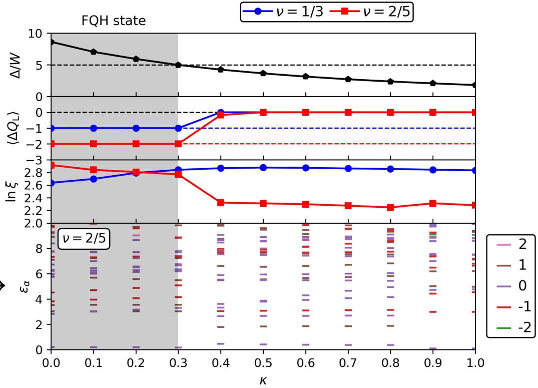

The orbital-polarized FQH states persist up to $\sim 30\%$ of the typical moiré hopping parameters, shown by the breakdown of the charge pumping and transition of the correlation length and entanglement spectrum. The persistent gap-to-width ratio shows that this is not due to gap closing but rather **induced orbital mixing**.

Summary

$$(t_1,t_2,t_2',\kappa)=(0.331,-0.01,0.097,1)$$

$$H_0=\underbrace{\boxed{\sum_{\langle ij\rangle}\left[t_1 e^{\mathrm{i}\theta_{ij}}\mathbf{c}_i^\dagger\cdot\mathbf{c}_j+\mathrm{H.c.}\right]}}_{\text{honeycomb Hofstadter}}+\kappa\underbrace{\boxed{\sum_{\langle ij\rangle_5}\left[t_2 e^{\mathrm{i}\theta_{ij}}\mathbf{c}_i^\dagger\cdot\mathbf{c}_j+t_2' e^{\mathrm{i}\theta_{ij}}(\mathbf{c}_i^\dagger\times\mathbf{c}_j)_z+\mathrm{H.c.}\right]}}_{\text{additional moiré contribution}}$$

If orbital-polarized fractional states can survive up to the same order of magnitude as typical hopping amplitudes in the moiré superlattice Hamiltonian, **what does this mean for other moiré superlattice Hamiltonians?**

- fractional states from underlying terms compete closely
- can predict fractional states from dominant terms in the Hamiltonian
- potential to tune hopping amplitudes to recover specific orbital-polarized fractional states

B. Andrews and A. Soluyanov, Phys. Rev. B **101**, 235312 (2020)

II. Higher-order Topology

Huaiqiang Wang
(visiting Uni. Zurich from Nanjing Uni.)

Apoorv Tiwari
(Uni. Zurich → KTH Stockholm)

Work in progress...

Motivation

- **Higher-order topological insulator (HOTI)** – new class of TIs whose $(d-1)$-dimensional boundary is also a TI, etc.
- Not all TIs can be used as building blocks to construct HOTIs, symmetries are crucial!

Many open questions:

- Generalization to *interacting* fermions? [Song et al., PRL 2017]
- HOTIs experimentally realized via hinge modes in bismuth ⇒ hexons for topological quantum computing? [Schindler et al., Nat Phys 2018]
- Can we numerically identify higher-order symmetry protected topology (HOSPTs)? [You et al., PRR 2020]

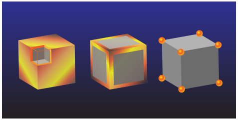

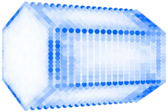

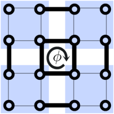

What is an SPT?

Historically: Measure local order parameter → spontaneous symmetry breaking → new phase of matter ✓

Nowadays: We know that topological phases have no local order parameter or spontaneous symmetry breaking...

SPT order	intrinsic topological order
• short-range entangled	• long-range entangled
• symmetry-protected boundary excitations	• topologically-protected boundary excitations
• “fractionalization” of symmetries	• fractionalization of charge
e.g. Haldane chain, TIs	e.g. FQHE, toric code

How to numerically detect SPTs

Formalism[4]

(canonical form)

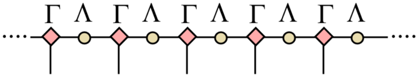

1. Obtain a ground-state wavefunction $|\Psi\rangle$ in an iMPS representation.
2. If $|\Psi\rangle$ is invariant under an internal symmetry, Σ, then the MPS cannot change (up to a phase): $\Sigma_{jj'}\Gamma_{j'} = e^{i\theta}U^{\dagger}\Gamma_j U$.
3. For a symmetry element g, the matrices U_g form a projective representation of the symmetry group.

e.g. for inversion symmetry $\mathcal{I} \Rightarrow \Gamma_j^{\intercal} = e^{i\theta}U_{\mathcal{I}}^{\dagger}\Gamma_j U_{\mathcal{I}}$

$\therefore$ we can distinguish SPT phases simply by checking if $U_{\mathcal{I}}U_{\mathcal{I}}^{*} = \pm\mathbf{1}$!

$\boxed{\text{We need to compute the } U \text{ matrices to detect SPTs}}$

[4] Pollmann and Turner, PRB **86**, 125441 (2012)

How to numerically detect SPTs

Formalism[4]

Generalized (right) transfer matrix

$$T^{\Sigma}_{\alpha\alpha';\beta\beta'} = \sum_j \left(\sum_{j'} \Sigma_{jj'} \tilde{\Gamma}_{j',\alpha\beta} \right) \Gamma^*_{j,\alpha'\beta'} \Lambda_\beta \Lambda_{\beta'}$$

The overlap of the symmetry transformation Σ with (right) Schmidt states corresponds to applying the generalized transfer matrix many times. Hence, only the dominant eigenvector (with eigenvalue=1) survives in the thermodynamic limit. Furthermore, **this dominant eigenvector is directly related to U due to the symmetry transformation**.

$$T^{\Sigma}_{\alpha\alpha';\beta\beta'} X_{\beta\beta'} = \eta X_{\alpha\alpha'} \xrightarrow{\text{for } |\eta|=1} \boxed{U_{\beta\beta'} = X^*_{\beta\beta'}}$$

[4] Pollmann and Turner, PRB **86**, 125441 (2012)

Bosonic SPT example in 1D

Spin-1 chain

↓↑↓↑... initial ansatz

Anisotropic Heisenberg model

$$H = J\sum_i \mathbf{S}_i \cdot \mathbf{S}_{i+1} + D\sum_i (S_i^z)^2$$

e.g. check if any phases are protected by the inversion symmetry

$$\mathcal{O}_\mathcal{I} = \begin{cases} 0 & \text{if } |\eta_\mathcal{I}| < 1 \\ \frac{1}{\chi}\mathrm{tr}(U_\mathcal{I} U_\mathcal{I}^*) & \text{if } |\eta_\mathcal{I}| = 1 \end{cases}$$

NB: this result can also be recovered by taking the limit of **partial reflections**.

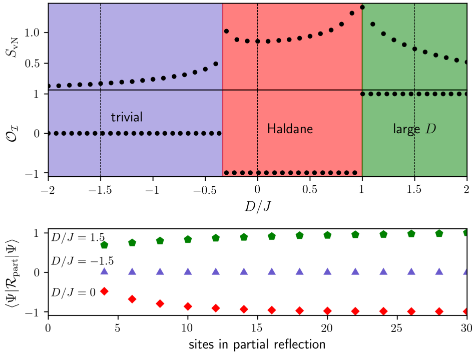

Fermionic SPT example in 1D

Su-Schrieffer-Heeger (SSH) model

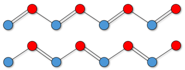

trivial

topological

Spinless SSH model

$$H = -t_1 \sum_j \left(c_j^{L\dagger} c_j^R + \text{H.c.} \right) - t_2 \sum_j \left(c_{j+1}^{L\dagger} c_j^R + \text{H.c.} \right)$$

symmetric under $\boxed{\mathcal{R} c_j^{L/R} \mathcal{R}^{-1} = c_{-j}^{R/L}}$ or $\boxed{\mathcal{R} c_j^{L/R} \mathcal{R}^{-1} = \mathrm{i} c_{-j}^{R/L}}$.

Order parameter

$$\boxed{\langle \mathcal{R}_{\text{part}} \rangle = \left(\prod_j \frac{1}{d_j} \right) e^{\mathrm{i}\theta}}$$

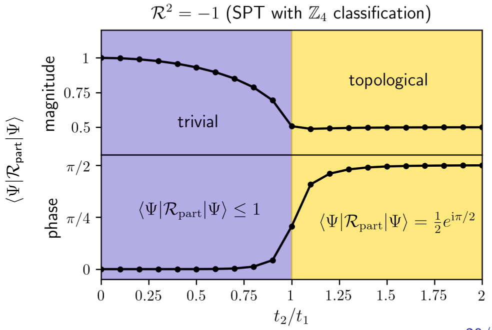

Higher-order SPTs

Strategy

SSH model: We used **partial reflections** to identify the projective representations of the overall *inversion* symmetry, which protects the edge modes.

Question: Can we use **partial rotations** in 2D systems to identify the projective representations of the overall *rotation* symmetry, which protects corner modes?

- ☐ Consider a C_4-symmetric model with symmetry-protected corner excitations
- ☐ Rotate only the central unit cell by $\tilde{C}_4$
- ☐ Is there an order parameter to identify the HOSPT?

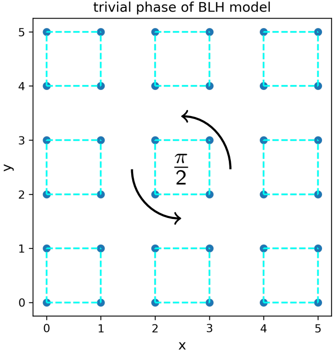

Higher-order SPTs

Benalcazar-Li-Hughes (BLH) model[5]

Intra-cell hopping, $\gamma \equiv \gamma_x = \gamma_y$

Inter-cell hopping, $\lambda \equiv \lambda_x = \lambda_y$

$$H = \sum_{\mathbf{R}} [\gamma (c^\dagger_{\mathbf{R},3} c_{\mathbf{R},1} + c^\dagger_{\mathbf{R},0} c_{\mathbf{R},2} + c^\dagger_{\mathbf{R},0} c_{\mathbf{R},1} + c^\dagger_{\mathbf{R},3} c_{\mathbf{R},2} + \mathrm{H.c.})$$
$$+ \lambda (c^\dagger_{\mathbf{R},3} c_{\mathbf{R}+\hat{\mathbf{x}},0} + c^\dagger_{\mathbf{R},2} c_{\mathbf{R}+\hat{\mathbf{x}},1} + c^\dagger_{\mathbf{R},1} c_{\mathbf{R}+\hat{\mathbf{y}},2} + c^\dagger_{\mathbf{R},3} c_{\mathbf{R}+\hat{\mathbf{y}},0} + \mathrm{H.c.})]$$

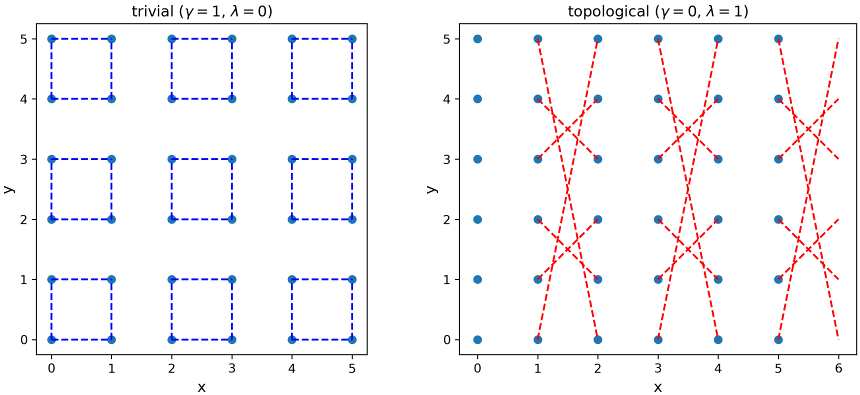

[5] BLH, PRB **99**, 245151 (2019)

Higher-order SPTs

BLH model: preliminary results

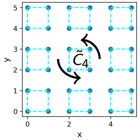

$C_4^4 = -1 \Rightarrow$

SPT with $\mathbb{Z}_8$ classification??

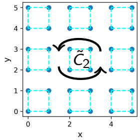

$C_4^4 = +1$ (SPT with $\mathbb{Z}_4$ classification?)

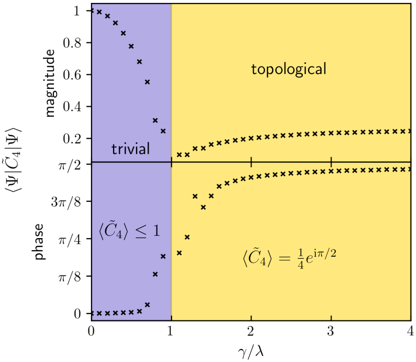

$C_2^2 = +1$ (no SPT detected)

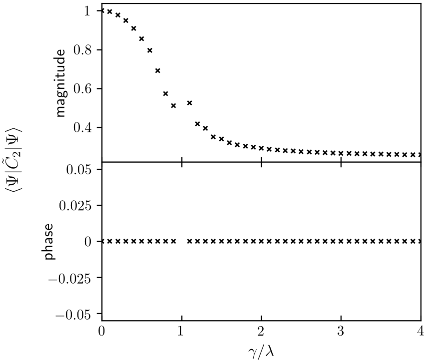

Summary

- Reviewed how to detect SPTs in 1D using matrix product states.
- Studied two examples of SPTs in 1D and showed how we can characterize them using **partial reflection**.
- Discussed how to generalize this concept to **partial rotation** for 2D systems with C_n symmetry.
- Presented preliminary results that identify the higher-order corner modes in the BLH model.

More possibilities to detect HOSPTs...

charge pumping

Fermionic tensor networks for higher-order topological insulators from charge pumping

Anna Hackenbroich,[1,2] B. Andrei Bernevig,[3,4] Norbert Schuch,[1,2] and Nicolas Regnault[3,5]
[1]*Max-Planck-Institute of Quantum Optics, Hans-Kopfermann-Str. 1, 85748 Garching, Germany*
[2]*Munich Center for Quantum Science and Technology, Schellingstraße 4, 80799 München, Germany*
[3]*Joseph Henry Laboratories and Department of Physics, Princeton University, Princeton, New Jersey 08544, USA*
[4]*Max-Planck-Institute of Microstructure Physics, 06120 Halle, Germany*
[5]*Laboratoire de Physique de l'École normale supérieure, ENS, Université PSL, CNRS, Sorbonne Université, Université Paris-Diderot, Sorbonne Paris Cité, 75005 Paris, France*

Regnault's group, PRB **101**, 115134 (2020)

higher-order entanglement

Higher-order entanglement and many-body invariants for higher-order topological phases

Yizhi You,[1] Julian Bibo,[2,3] and Frank Pollmann[2,3]
[1]*Princeton Center for Theoretical Science, Princeton University, New Jersey 08544, USA*
[2]*Department of Physics, Technical University of Munich, 85748 Garching, Germany*
[3]*Munich Center for Quantum Science and Technology (MQCST), D-80799 Munich, Germany*

Pollmann's group, PRR **2**, 033192 (2020)

Outlook

Moiré Materials [B. Andrews and A. Soluyanov, PRB **101**, 235312 (2020)]

Open question: can we effectively interface with ab-initio calculations by Wannierization?
Future directions: fractional Chern insulators, higher-order filling factors, non-Abelian states, stability in the continuum limit, . . .

Higher-order Topology [Work in progress...]

Open question: can we generally classify HOSPTs via partial symmetry transformations?
Future directions: interacting and driven systems, PEPS implementation, entanglement spectroscopy, real materials, . . .

Thank you for listening!

Supplementary Slides

Additional References

1. Edge-state counting:
   Wen, Int J Mod Phys B **6**, 1711–1762 (1992)
2. Need for C_4 symmetry in the BBH model:
   Lin & Hughes, PRB **98**, 241103 (2018)
3. Cobordism classification:
   Shiozaki et al., PRB **95**, 205139 (2017)
4. Many-body invariants for fermionic SPTs:
   Shapourian et al., PRL **118**, 216402 (2017)
5. Interacting HOTI:
   Song et al., PRL **119**, 246402 (2017)
6. Floquet HOTI:
   Rodriguez-Vega et al., PRB **100**, 085138 (2019)
7. AFM corner modes with interactions:
   arXiv:2101.05058 [cond-mat.str-el]

Alexey's Legacy

Z2Pack

Wannier Tools®

PHYSICAL REVIEW B **83**, 035108 (2011)

Wannier representation of $\mathbb{Z}_2$ topological insulators

Alexey A. Soluyanov* and David Vanderb
Department of Physics and Astronomy, Rutgers University, Piscataway,
(Received 7 September 2010; revised manuscript received 3 December 20

PHYSICAL REVIEW B **83**, 235401 (2011)

Computing topological invariants without inversion symmetry

Alexey A. Soluyanov* and David Vanderbilt†
Department of Physics and Astronomy, Rutgers University, Piscataway, New Jersey 08854-0849, USA
revised manuscript received 18 April 2011; published 2 June 2011)

LETTER

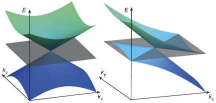

doi:10.1038/nature15768

Type-II Weyl semimetals

Alexey A. Soluyanov[1], Dominik Gresch[1], Zhijun Wang[2], QuanSheng Wu[1], Matthias Troyer[1]

PHYSICAL REVIEW B **93**, 115317 (2016)

Optimizing spin-orbit splittings in InSb Majorana nanowires

Alexey A. Soluyanov, Dominik Gresch, and Matthias Troyer
Theoretical Physics and Station Q Zurich, ETH Zurich, 8093 Zurich, Switzerland

Roman M. Lutchyn, Bela Bauer, and Chetan Nayak
rosoft Research, Santa Barbara, California 93106, USA
ised manuscript received 25 February 2016; published 29 March 2016)

LETTER

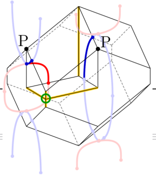

doi:10.1038/nature19099

Nodal-chain metals

Tomáš Bzdušek[1], QuanSheng Wu[1,2], Andreas Rüegg[1], Manfred Sigrist[1] & Alexey A. Soluyanov[1,2,3]

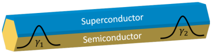

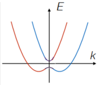

Motivation

moiré superstructures are an exciting challenge

- ✓ demonstrated success in experiments
- ✓ high potential for customization
- ✓ configurable way of accessing fractional states

- ✗ moiré unit cell is typically large
- ✗ experiments are delicate
- ✗ disputed claims for certain exotic phases

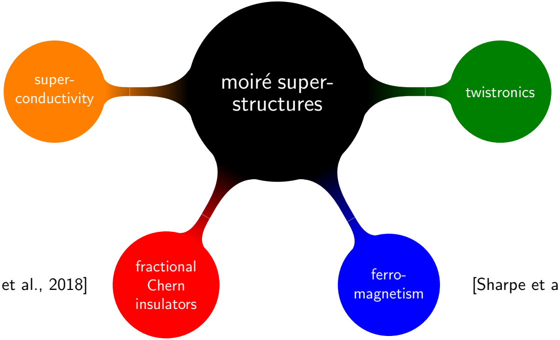

[Cao et al., 2018]

[Carr et al., 2016]

[Spanton et al., 2018]

[Sharpe et al., 2019]

Numerical Method

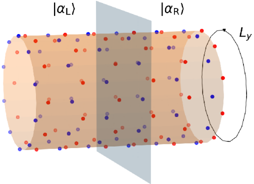

We perform our calculations using **infinite density matrix renormalization group (iDMRG)** on a **thin cylinder** geometry[3] with TeNPy[4].

1. Initial wavefunction transcribed to MPS (winding around cylinder).
2. Decompose the wavefunction $|\psi\rangle = \sum_\alpha \Lambda_\alpha |\alpha_\mathrm{L}\rangle \otimes |\alpha_\mathrm{R}\rangle$ into two half-cylinders up to bond dimension χ.
3. Schmidt eigenspace $\Rightarrow$ reduced density matrix eigenspace.
4. Von Neumann entanglement entropy: $S_\mathrm{vN} = -\sum_\alpha \Lambda_\alpha^2 \log \Lambda_\alpha^2$.
5. Iterating until convergence of S yields a ground-state MPS $|\psi\rangle$.

Semi-thermodynamic limit and no band projection needed ✓

[3] Cincio and Vidal, PRL **110**, 067208 (2013)

[4] Hauschild and Pollmann, SciPost Phys. Lect. Notes, 5 (2018)

Numerical Method

TeNPy configuration

Lattice

`class MagneticHoneycomb(Lattice)`

Model

`class FermionicHex1Hex5OrbitalModel(CouplingMPOModel)`

Initial state

`product_state = ['full_x full_y'] + [0]*29`

DMRG parameters

`dmrg_params = {'mixer': True, 'max_E_err': 1.e-10, 'max_S_err': 1.e-8, ...}` (No `'max_sweeps'` set)

Lattice geometries

Example: $\nu = 1/3$ state

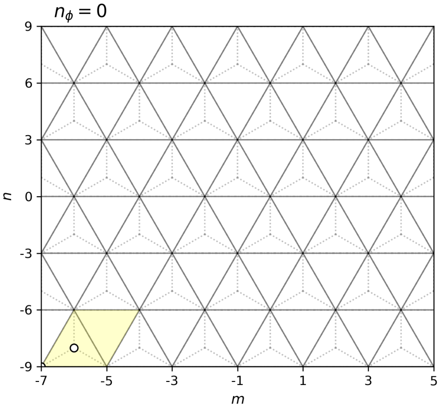

We start with the unit cell on the moiré superlattice, with two orbitals per site.

$$\# \text{ lattice sites} = 2$$

$$\# \text{ orbital sites} = 4$$

Lattice geometries

Example: $\nu = 1/3$ state

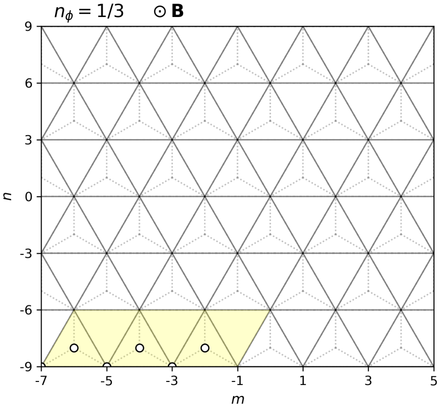

In the presence of a perpendicular magnetic field, Landau gauge, $\mathbf{A} = Bx\hat{\mathbf{e}}_y$, extends the unit cell in the x-direction: $1 \times 1 \rightarrow q \times 1$.

$\#$ lattice sites $= 6$

$\#$ orbital sites $= 12$

Lattice geometries

Example: $\nu = 1/3$ state

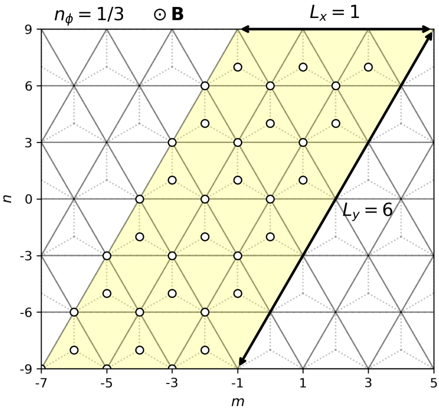

We can build our system by adding magnetic unit cells along the cylinder circumference (or axis).

$\#$ lattice sites $= 36$

$\#$ orbital sites $= 72$

Lattice geometries

Example: $\nu = 1/3$ state

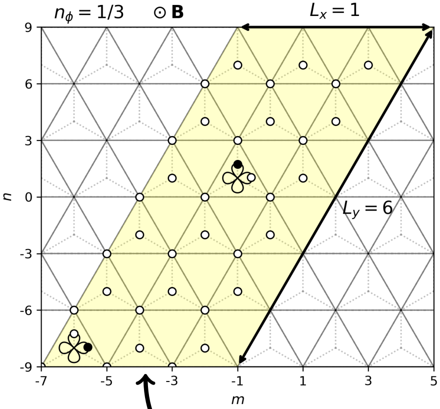

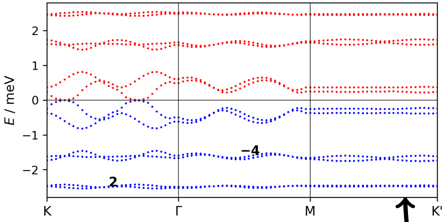

Orbital polarization ⇒ two quasi-degenerate $C = 1$ bands.

lattice sites = 36

orbital sites = 72

We expect a FQH state at filling

$$\nu = \frac{r}{|kC|r+1} \stackrel{!}{=} \frac{1}{2 \times 1 + 1} = \frac{1}{3}$$

of the lowest quasi-degenerate band.

This corresponds to filling $1/36$ of the orbital sites in our system.

Lattice geometries

Example: $\nu = 2/5$ state

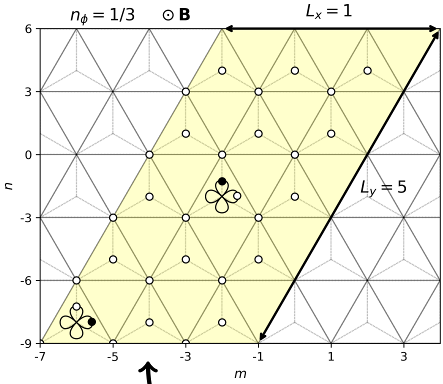

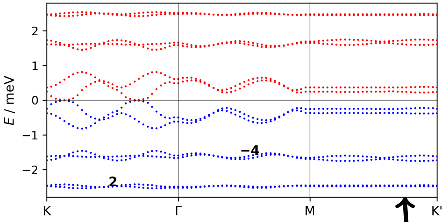

Orbital polarization $\Rightarrow$ two quasi-degenerate $C = 1$ bands.

We expect a FQH state at filling

$$\nu = \frac{r}{|kC|r + 1} \stackrel{!}{=} \frac{2}{2 \times 2 + 1} = \frac{2}{5}$$

of the lowest quasi-degenerate band.

$\#$ lattice sites $= 30$

$\#$ orbital sites $= 60$

This corresponds to filling $1/30$ of the orbital sites in our system.

Evidence for the $\nu = 2/5$ state

...from flux insertion[6]

Charge pumping

Total charge pumped across the cut in the cylinder corresponds to the Hall conductivity $\sigma_{\mathrm{H}} \propto C\nu$. ✓

Spectral flow

Entanglement energies flow into themselves after the insertion of s flux quanta, with the charge sector labeling shifted by $|C|r$. ✓

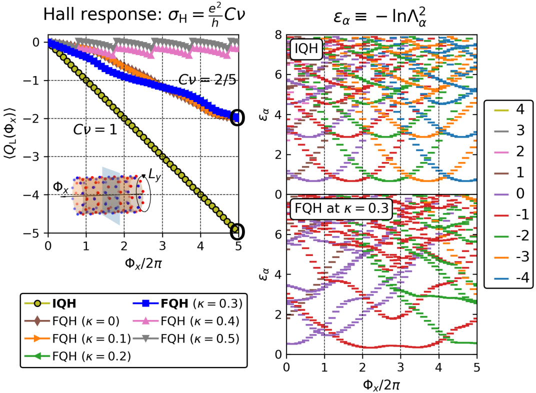

[6] Andrews and Soluyanov, PRB **101**, 235312 (2020)

Evidence for the $\nu = 2/5$ state(?)

...from entanglement[8]

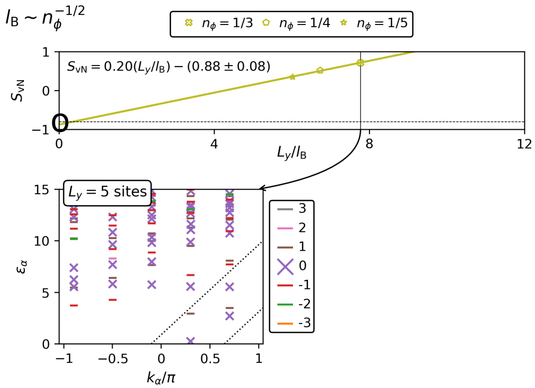

Entanglement scaling

From the 'area law':

$$S = cL_y - \gamma,$$

the topological entanglement entropy is given as

$$\gamma = \ln \sqrt{\sum_i d_i^2},$$

with $d_i = 1$ for Abelions. $\sim$

Edge counting

Conformal field theory predicts the ground-state counting $\{1, 2, 5, 10, \dots\}$ for each Q_L sector. $\sim$

[8] Andrews et al., PRB **103**, 075132 (2021)

Why the transition?

A: The induced orbital mixing in the moiré Hamiltonian.

- gap-to-width ratio decreases with increasing κ, suppressing the role of interactions. However, $\Delta/W \sim 5$ and interactions are still large.
- as the orbital-mixing parameter is increased, the lowest two bands can no longer be treated as quasi-degenerate $C = 1$ bands.
- for the $\nu = 1/3$ state, a system filling of $^{1}/_{36}$ would now correspond to $\nu = 1/6$ for the composite band pair. This is not a hierarchy state.
- for the $\nu = 2/5$ state, a system filling of $^{1}/_{30}$ would now correspond to $\nu = 1/5$ for the composite band pair. This is a hierarchy state, however not stabilized under these parameters.
- this does not exclude the possibility of stable hierarchy states with $\kappa = 1$. These states could still be realized with different fillings, band parameters, flux densities or interaction strengths.

Summary

- Analyzed the breakdown of orbital-polarized hierarchy states as orbital mixing is induced in the moiré Hamiltonian.
- Polarized states can survive up to $\sim 30\%$ of the moiré hopping amplitudes, since the original orbital-mixing term is small.
- Shows that FQH states in realistic moiré flatband systems have close competition from their orbital-polarized counterparts.

Latest advancements...

Hamiltonian compression

Efficient simulation of moiré materials using the density matrix renormalization group

Tomohiro Soejima (副島智大),[1,*] Daniel E. Parker,[1,*] Nick Bultinck,[1,2] Johannes Hauschild,[1] and Michael P. Zaletel[1,3]
[1]Department of Physics, University of California, Berkeley, California 94720, USA
[2]Department of Physics, Ghent University, 9000 Ghent, Belgium
[3]Materials Sciences Division, Lawrence Berkeley National Laboratory, Berkeley, California 94720, USA

Zaletel's group, PRB **102**, 205111 (2020)

twisted double bilayers

Gate-Tunable Fractional Chern Insulators in Twisted Double Bilayer Graphene

Zhao Liu,[1,*] Ahmed Abouelkomsan,[2,†] and Emil J. Bergholtz[2,‡]
[1]Zhejiang Institute of Modern Physics, Zhejiang University, Hangzhou 310027, China
[2]Department of Physics, Stockholm University, AlbaNova University Center, 106 91 Stockholm, Sweden

(Received 26 April 2020; accepted 11 December 2020; published 12 January 2021)

Bergholtz's group, PRL **126**, 026801 (2021)

Fermionic SPT example in 1D

Su-Schrieffer-Heeger (SSH) model

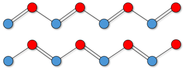

Spinless SSH model

$$H = -t_1 \sum_j \left(c_j^{L\dagger} c_j^R + \text{H.c.} \right) - t_2 \sum_j \left(c_{j+1}^{L\dagger} c_j^R + \text{H.c.} \right)$$

symmetric under $\boxed{\mathcal{R} c_j^{L/R} \mathcal{R}^{-1} = c_{-j}^{R/L}}$ or $\boxed{\mathcal{R} c_j^{L/R} \mathcal{R}^{-1} = \mathrm{i} c_{-j}^{R/L}}$.

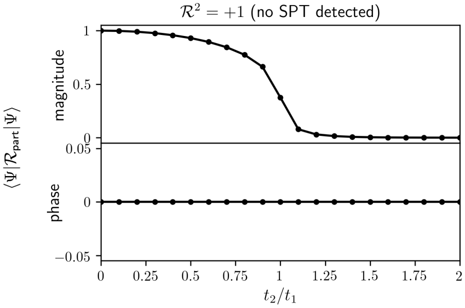

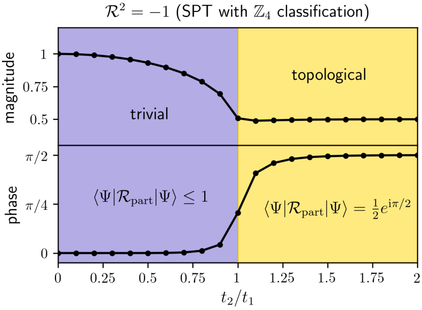

Fermionic SPT example in 1D

Su-Schrieffer-Heeger (SSH) model

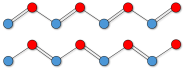

Spinless SSH model

$$H = -t_1 \sum_j \left(c_j^{L\dagger} c_j^R + \text{H.c.} \right) - t_2 \sum_j \left(c_{j+1}^{L\dagger} c_j^R + \text{H.c.} \right)$$

Order parameter

$$\boxed{\langle \mathcal{R}_{\text{part}} \rangle = \left(\prod_j \frac{1}{d_j} \right) e^{i\theta}}$$

$\mathcal{R}^2 = -1$ (SPT with $\mathbb{Z}_4$ classification)

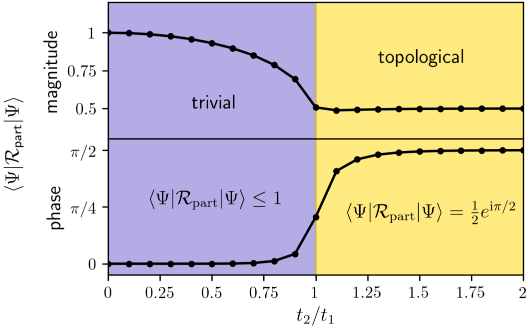

Higher-order SPTs
Strategy

SSH model: We used **partial reflections** to identify the projective representations of the overall *inversion* symmetry, which protects the edge modes.
Question: Can we use **partial rotations** in 2D systems to identify the projective representations of the overall *rotation* symmetry, which protects corner modes?

- ☐ Consider a C_4-symmetric model with symmetry-protected corner excitations
- ☐ Rotate only the central unit cell by $\tilde{C}_4$
- ? Is there an order parameter to identify the HOSPT?

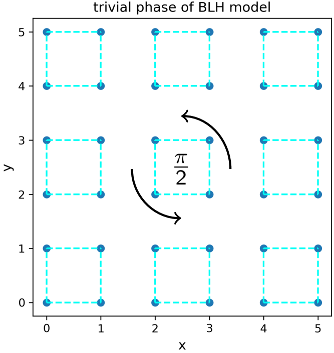

Higher-order SPTs
Strategy

SSH model: We used **partial reflections** to identify the projective representations of the overall *inversion* symmetry, which protects the edge modes.

Question: Can we use **partial rotations** in 2D systems to identify the projective representations of the overall *rotation* symmetry, which protects corner modes?

- ☐ Consider C_4-symmetric model with symmetry-protected corner excitations.
- ☐ Rotate only the central unit cell by $\tilde{C}_4$.
- ? Is there an order parameter to identify the HOSPT?
- ? How do we implement this using DMRG?

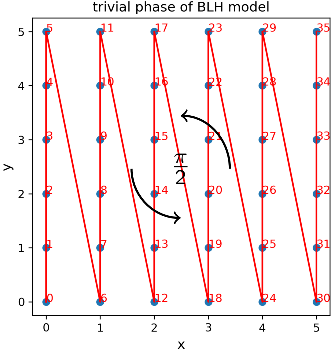

Higher-order SPTs

Numerical method

For the SSH chain, we performed the reflection using an algorithm that sweeps left-to-right, while performing **two-site swap gates**.

$\mathcal{R}^2 = +1$

n_L	n_R	amplitude
0	0	1
0	1	1
1	0	1
1	1	-1

$\mathcal{R}^2 = -1$

n_L	n_R	amplitude
0	0	1
0	1	$-\mathrm{i}$
1	0	$-\mathrm{i}$
1	1	$(-\mathrm{i})^2(-1) = 1$

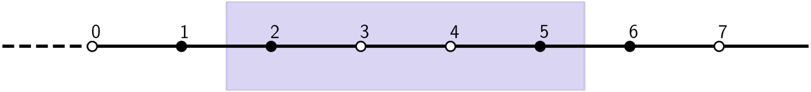

Analogously, we can engineer multi-site swap gates for the 2D system such that $C_4^4 = \pm 1$ is satisfied.

Higher-order SPTs
Numerical method

For the SSH chain, we performed the reflection using an algorithm that sweeps left-to-right, while performing **two-site swap gates**.

$\mathcal{R}^2 = +1$

n_L	n_R	amplitude
0	0	1
0	1	1
1	0	1
1	1	-1

$\mathcal{R}^2 = -1$

n_L	n_R	amplitude
0	0	1
0	1	$-\mathrm{i}$
1	0	$-\mathrm{i}$
1	1	$(-\mathrm{i})^2(-1) = 1$

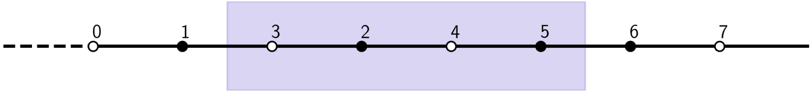

Analogously, we can engineer multi-site swap gates for the 2D system such that $C_4^4 = \pm 1$ is satisfied.

Higher-order SPTs

Numerical method

For the SSH chain, we performed the reflection using an algorithm that sweeps left-to-right, while performing **two-site swap gates**.

$\mathcal{R}^2 = +1$

n_L	n_R	amplitude
0	0	1
0	1	1
1	0	1
1	1	-1

$\mathcal{R}^2 = -1$

n_L	n_R	amplitude
0	0	1
0	1	$-\mathrm{i}$
1	0	$-\mathrm{i}$
1	1	$(-\mathrm{i})^2(-1) = 1$

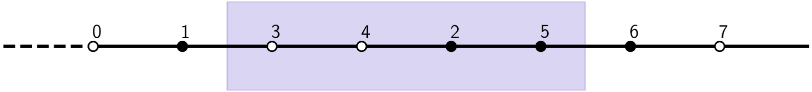

Analogously, we can engineer multi-site swap gates for the 2D system such that $C_4^4 = \pm 1$ is satisfied.

Higher-order SPTs
Numerical method

For the SSH chain, we performed the reflection using an algorithm that sweeps left-to-right, while performing **two-site swap gates**.

$\mathcal{R}^2 = +1$

n_L	n_R	amplitude
0	0	1
0	1	1
1	0	1
1	1	-1

$\mathcal{R}^2 = -1$

n_L	n_R	amplitude
0	0	1
0	1	$-\mathrm{i}$
1	0	$-\mathrm{i}$
1	1	$(-\mathrm{i})^2(-1) = 1$

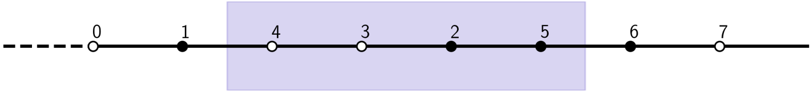

Analogously, we can engineer multi-site swap gates for the 2D system such that $C_4^4 = \pm 1$ is satisfied.

Higher-order SPTs

Numerical method

For the SSH chain, we performed the reflection using an algorithm that sweeps left-to-right, while performing **two-site swap gates**.

$\mathcal{R}^2 = +1$

n_L	n_R	amplitude
0	0	1
0	1	1
1	0	1
1	1	-1

$\mathcal{R}^2 = -1$

n_L	n_R	amplitude
0	0	1
0	1	$-\mathrm{i}$
1	0	$-\mathrm{i}$
1	1	$(-\mathrm{i})^2(-1) = 1$

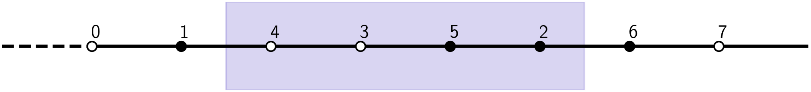

Analogously, we can engineer multi-site swap gates for the 2D system such that $C_4^4 = \pm 1$ is satisfied.

Higher-order SPTs

Numerical method

For the SSH chain, we performed the reflection using an algorithm that sweeps left-to-right, while performing **two-site swap gates**.

$\mathcal{R}^2 = +1$

n_L	n_R	amplitude
0	0	1
0	1	1
1	0	1
1	1	-1

$\mathcal{R}^2 = -1$

n_L	n_R	amplitude
0	0	1
0	1	$-\mathrm{i}$
1	0	$-\mathrm{i}$
1	1	$(-\mathrm{i})^2(-1) = 1$

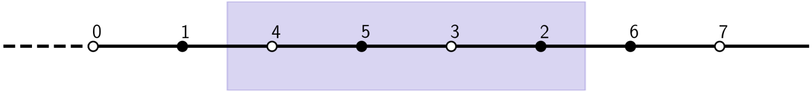

Analogously, we can engineer multi-site swap gates for the 2D system such that $C_4^4 = \pm 1$ is satisfied.

Higher-order SPTs
Numerical method

For the SSH chain, we performed the reflection using an algorithm that sweeps left-to-right, while performing **two-site swap gates**.

$\mathcal{R}^2 = +1$

n_L	n_R	amplitude
0	0	1
0	1	1
1	0	1
1	1	-1

$\mathcal{R}^2 = -1$

n_L	n_R	amplitude
0	0	1
0	1	$-\mathrm{i}$
1	0	$-\mathrm{i}$
1	1	$(-\mathrm{i})^2(-1) = 1$

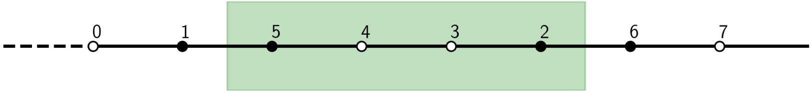

Analogously, we can engineer multi-site swap gates for the 2D system such that $C_4^4 = \pm 1$ is satisfied.

Higher-order SPTs

BLH model[10]: key features

- ☐ C_4-protected corner modes in the topological regime.

$\gamma < \lambda$

- ☐ Trivial regime ($\gamma > \lambda$): insulator at $1/4$ filling.
  Topological regime ($\gamma < \lambda$): insulator at $1/2$ filling.

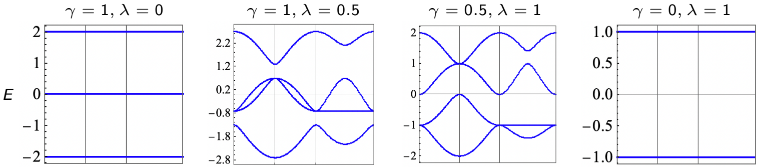

[10] BLH, PRB **99**, 245151 (2019)

Stability of FCIs in the Effective Continuum Limit of $|C| > 1$ Harper-Hofstadter Bands

Bartholomew Andrews & Gunnar Möller

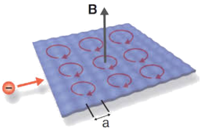

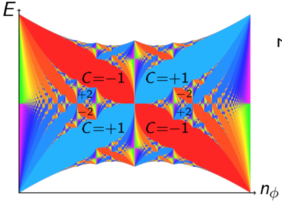

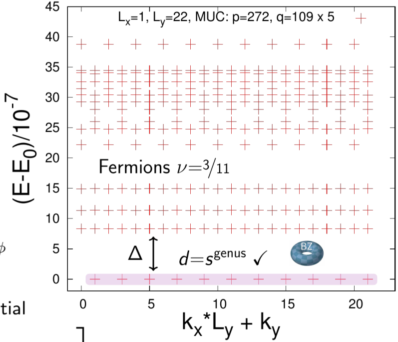

$$H = \sum_{i,j} \left[\underbrace{t_{ij}}_{\text{hopping parameter}} \overbrace{e^{\phi_{ij}}}^{\text{magnetic translation-invariant phase}} c_j^\dagger c_i + \text{h.c.} \right] + \underbrace{\mathcal{P}_{\text{LB}}}_{\text{lowest-band projection operator}} \left[\sum_{i<j} \overbrace{V_{ij}}^{\text{interaction potential}} :\rho(\mathbf{r}_i)\rho(\mathbf{r}_j): \right] \mathcal{P}_{\text{LB}}$$

bosons $\Rightarrow$ contact int
fermions $\Rightarrow$ NN int

Using ED, we explore CF series $\nu = \frac{r}{|kC|r+1}$ for higher Chern number.

What's new?

stable FCIs in bands with $|C| > 1$

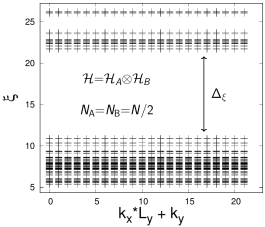

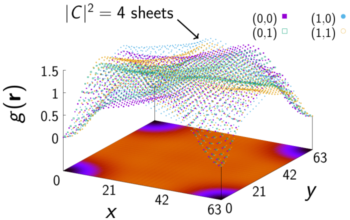

$|C|^2$ correlation sheets

charge density instabilities

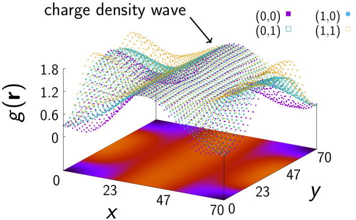

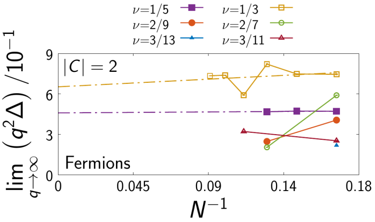

robust $|C| > 1$ thermo cont limits